MANSOURA JOURNAL OF CHEMISTRY
Official Journal of Faculty of Science, Mansoura University, Egypt
E-mail: scimag@mans.edu.eg ISSN: 2974-4938

Removal of Aniline Blue and Methyl Violet from Solution using Chitosan/Biomass Based Activated Carbon Composite from Eggplant and Pomegranate peels

Farida M.S.E. El Dars*, Aya E. Nouh and Sahar K Mohamed,

Chemistry Department, Faculty of Science, Helwan University, Ain Helwan, Helwan, Cairo 11795, Egypt

**Corresponding author. Email: fkeldars@aucegypt.edu*

Received: 16/11/2019
Accepted: 1/12/2019

Abstract: In this work, the removal of aniline blue (AB) and methyl violet (MV) from aqueous solution using chitosan (Cs) and chitosan/activated carbon biomass prepared from eggplant (CS/AC_E) and pomegranate peels (Cs/AC_P) was investigated. The respective Cs/biomass was formed from the carbonized eggplant and pomegranate peels which was activated with 0.1 M $ZnCl_2$ prior to their incorporation. The dye removal process was studied in batch system with respect to the initial pH, contact time, temperature, adsorbent weight and the initial dye concentration. The results indicated that optimal (AB) and (MV) removal was achieved at pH_5 and after 5 h contact time. The experimental data was best fitted to pseudo-second-order model for both dyes based upon the obtained R^2 values. As well, the process followed the Freundlich isotherm model. The thermodynamic parameters (ΔH^o, ΔS^o and ΔG^o) for the prepared adsorbents uptake of both dyes indicated that the process was endothermic and spontaneous for AB, however, it was non spontaneous for MV.

keywords: Chitosan / biomass, eggplant and pomegranate peel activated carbon, aniline blue, and methyl violet.

1.Introduction

One of the major environmental problems is the discharge of residual dyes from the textile industries which are difficult to remove by traditional treatment methods [1]. This organic load is hazardous and does pose threats to human and other living organisms in the environment. Generally, if this wastewater is discharged into water resources, it will deplete the dissolved oxygen content and inhibit sunlight from penetrating into these water bodies thus hindering photosynthesis [2]. In addition to that, dye molecules have significantly high molecular weights plus a complex structure which makes them non-biodegradable [3]. Several techniques, such as chemical oxidation, flocculation, precipitation, membrane filtration, biodegradation and electrochemical techniques have been employed for dyes and color removal [4]. However, these methods have several drawbacks such as high cost, low removal effectivity as well as do lead to the generation large amounts of hazardous sludge.

Adsorption, on the other hand, is highly efficient and economical method for the removal of dyes from wastewater [4]. As well, activated carbon (AC) has been widely used as adsorbent for treatment of industrial wastewaters due to its efficiency and economic feasibility. However, the ability of activated carbons to adsorb pollutants from aqueous solutions depends upon the nature of organic material used and the method of activation [5]. Nonetheless, selection of this material is based upon cost, effectiveness, availability and final adsorptive properties of the adsorbent to remove pollutants compounds from wastewaters [6]. As well, the need for eco-adsorbents that are both non-toxic and that do possess high surface area has led to the exploration of some agricultural wastes. This has reduced the associated costs and lead to the sustainable management of these wastes.

Chitosan has been used in water treatment, seed treatment as well as in other environmental applications. Chitosan derivatives have also have gained wide

attention as effective biosorbent because of their low cost and high content of amino and hydroxyl functional groups which have significant adsorption potential for the removal of various wastewater contaminated with dyes [7]. Moreover, incorporation of activated carbon with chitosan polymer has been reported [8, 9]. Such chitosan composites were shown to be effective in adsorption and removal of Cd^{2+} [10] and in treatment of water containing organic micro-pollutants [11].

In this study, modified chitosan/activated carbon composites were prepared using abundant agriculture/ produce waste. This work aims to investigate the efficiency of the prepared composite biomass in the removal of selected organic dyes from solution, namely: aniline blue (AB) and methyl violet (MV).

2. Materials

2.1. Sorbent materials preparation

2.1.1. Activated carbon:

eggplant and pomegranate peels were obtained locally and used to prepare activated carbon (AC_E and AC_P) for incorporation with chitosan to form the Cs/ AC composite. Before use, both peels were washed separately and thoroughly to remove any dirt then dried, crushed and sifted through 60-mesh sieve. The process of activation of the carbonized peels was done as per the following procedure [12]. 200 g of the dried eggplant and pomegranate peels were individually stirred in a boiling solution of anhydrous $ZnCl_2$ (0.1 M) (100 g/ 1 L distilled H_2O) for 1h. The solution was filtered and the filtrate was dried at 60 ºC for 12 h. Carbonization of this filtrate was done in a muffle furnace at 500 ºC for 2h. After cooling, the prepared activated carbon was washed with distilled H_2O to remove excess $ZnCl_2$ until a neutral pH was reached.

2.1.2. Chitosan: Chitosan powder from crab shells (Cs) (Poly-(1.4-B-D-glucopyranosamine); 2-Amino-2-deoxy-(1->4)-B-D-glucopyranan) was obtained from ROTH-Germany.

2.1.3. Preparation of chitosan/activated carbon biomass:

Solution (1): 0.4 g chitosan (Cs) was dissolved in 15 mL of 2% CH_3COOH (El-Nasr Pharmaceutical Company-Cairo, Egypt).

Solution (2): 0.1 g of AC_E and AC_P were immersed in 10 mL of 2% acetic acid solution and sonicated for ½ h. To prepare the chitosan /activated carbon biomass, solution (1) and solution (2) were mixed together while stirring for ½ h. The homogenized chitosan-activated carbon biomass (Cs/AC_E and Cs/AC_P) solutions were then poured into 5-cm Petri dishes and left to dry in an oven for 6 h at 60 ºC. The prepared activated carbon was then washed with distilled H_2O until a neutral pH was reached.

2.1.4. Characterization of the prepared Chitosan/ activated carbon biomass:

Characterization of the prepared adsorbent materials was carried out using the following techniques: FTIR spectroscopy (FTIR (6100 JASCO, Japan) with KBr pellets (4000–400 cm^{-1}) with spectral resolution of 4 cm^{-1}, XRD: BruckerD8 Advanced (Germany) with Cu target (1.5406 Å) at 2θ scanning range from 4º to 70º.

2.3. Preparation of selected dye solutions

- Aniline blue (AB)($C_{32}H_{25}N_3O_9S_3Na_2$)(pka= 4.6) was obtained from Alfa For Laboratory Fine Chemicals (Germany). This acidic dye is an organic soluble compound utilized in textile industry for the dyeing of nylon, wool, silk and cotton fibers. However, it has a long residence time in water [13].

- Methyl violet (MV) ($C_{24}H_{28}N_3Cl$) (pka = 0.9) was purchased from Sigma–Aldrich (England). While it is used abundantly in textile dyeing because it is very cheap, it is known to possess carcinogenic and mutagenic properties.

- Stock solutions of AB dye and MV (1000 mg/L) were prepared by dissolving the required mass in 1L of distilled water.

2.4. Buffer solutions

Buffer solutions required for testing pH solution were prepared as follows: pH (1-2): KCl (0.2 M) + HCl (0.2 M); pH (3-5): citric acid (0.1 M) + sodium citrate dihydrogen (0.1 M); pH (6-8): sodium dihydrogen phosphate (0.2 M) + disodium hydrogen phosphate (0.2 M); pH (9): ammonium chloride (0.3 M) + ammonia solution (28 %). All pH measurements and adjustments were conducted using Jenway 3310 pH-Meter.

2.5. Adsorption and optimization experiments.

Batch adsorption experiments were carried out in a thremostated water bath/shaker at a constant shaking rate. During these experiments, the effect of contact time, concentration, solution pH, adsorbent dose and temperature upon dye uptake was investigated. 50 mL of dye solution of known concentrations (10-150 mg/L) were shaken with different adsorbent weights (0.0125-0.1 g), at different temperatures (25- 40 ºC), at variable contact time (15- 300 min) and at pH (1-9). After each defined period, the mixture was centrifuged at 4000 rpm for 10-15 min then filtered. The filtrate was analyzed for the remaining dye concentrations (AB at λ_{max}= 463.5 nm and MV at λ_{max} =584.5 nm) using JASCO V-630 UV-Vis spectrophotometer (Japan).

The percentage dye removal (%) was calculated as follows:

$$\% \text{ removal} = [C_0 - C_f / C_0] \times 100 \quad (1)$$

where C_0 and C_t are the initial and final concentration of the dye in solution (mg/L). The amount of dye accumulated per unit mass of adsorbent was calculated according to the following equation:

$$q_t = (C_0 - C_t)\, V / m \quad (2)$$

where m is the weight of sorbent used (g) and V is the volume of dye solution (L). At equilibrium, contact time becomes t_e, C_t becomes C_e and the amount of dye sorbed (q_t) is equivalent to amount at equilibrium (q_e).

3. Result and discussion

3.1 Characterization of adsorbent:

Figure 1 shows the XRD patterns obtained for Cs, AC_E, AC_P, Cs/AC_E and Cs/AC_p, respectively**.** Cs scan exhibited a broad diffraction peak at 2θ = 20, which is typical of a semi-crystalline chitosan [5]. Both AC_E and AC_P had two broad peaks at 2θ = 20–30° and 40–50° which may be attributed to the reflection from the (0 0 2) and (1 0 0) planes. These broad peaks are characteristic of amorphous carbon containing carbon ring that was disorderly stacked up [8]. Also, the addition of activated carbon on chitosan film for both Cs/AC_E and Cs/AC_p resulted in an amorphous chitosan film. This amorphous phase was deemed favorable for the adsorption process as the active sites become more accessible for the adsorbate [10]. As well, impregnation of activated carbon within the chitosan film increased its overall crystallinity and thus many sharp peaks with different intensities were observed by XRD [10].

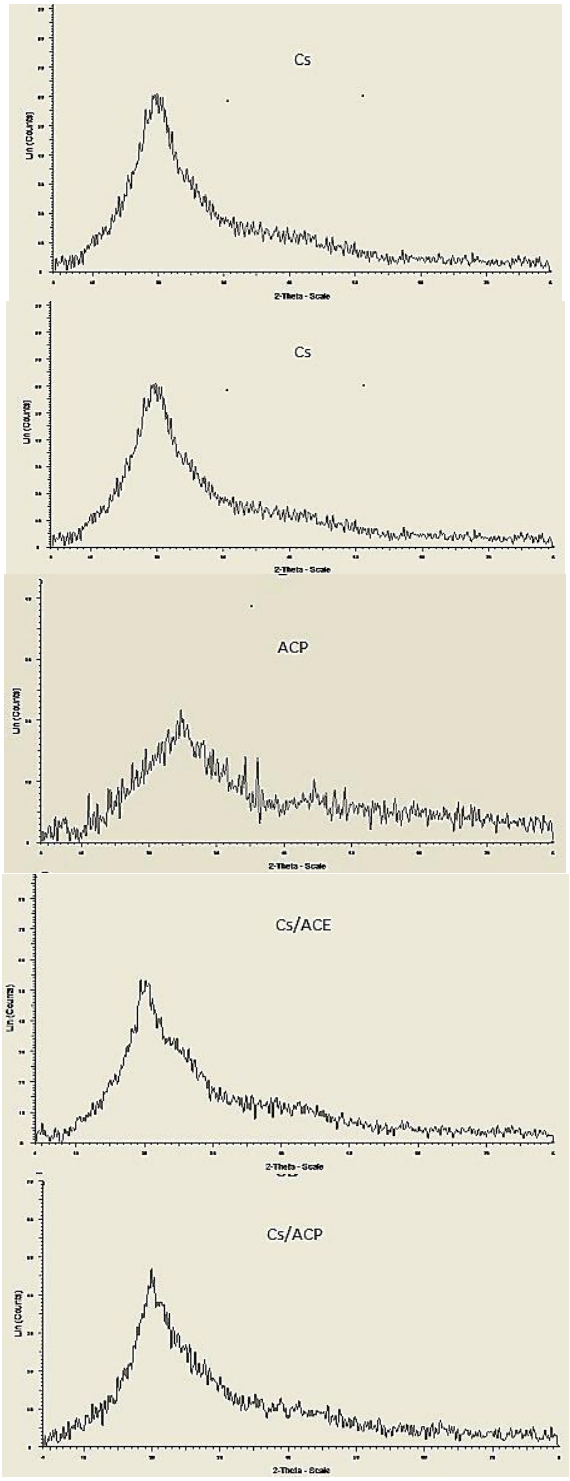

Figure.1.XRD for Cs, AC_E, AC_P, Cs/AC_E and Cs/AC_P

Figure 2 shows the characteristic functional groups of Cs, AC_E, AC_P, Cs/AC_E and Cs/AC_P, respectively, identified with FTIR. Functional

groups like C=O (H bonded) and N–H (1º amide) bending vibrations were reported to be responsible for the increase in adsorption efficiency [12]. **C**hitosan biopolymers showed peaks at 3429.78 cm^{-1} which are associated with the stretching vibrations of –OH and the aliphatic C-H stretching at 2927.41 cm^{-1}. Peaks observed at 1636.3 cm^{-1} are associated with N-H bend in the $NHCOCH_3$ group (Amid I band) and that at 1425.14 cm^{-1} with C-C stretch in ring. The peak at 1183.11 cm^{-1} may be assigned to the anti- symmetric stretching of (C–O) bridge and that at 1026.91 cm^{-1} reflects the skeletal vibration involving C–N stretching. The peak at 669.178 cm^{-1} is associated with the presence of -C=C-H : C-H bending [12].

For **AC_E**, the peak at 3432.67 cm^{-1} reflect the O-H group surface functional groups present in the granular activated carbon. The band at 2924.52 cm^{-1} corresponds to the aliphatic C-H stretching. Peaks at 1630.52 cm^{-1} are attributed to Amide I band which are associated with the occurrence of (N-H) bending; peak at 594.93cm^{-1} may be attributed to C-Br stretching. **Cs/AC_E** showed a peak at 3433.64 cm^{-1} which may be due to the O–H (H bonded) stretching. The peak at 2923.56 cm^{-1} corresponds to the typical asymmetric and symmetric stretching of C-H stretch and the corresponding vibrations for N-H bends and O-H in plane bending were observed at 1635.34 cm^{-1} and 1384.64 cm^{-1}, respectively. Peaks at 1065.48 cm^{-1} and 610.36 cm^{-1} are associated with the presence of C-N stretching and -C=C-H: C-H bending.

AC_P showed a peak at 3432.67 cm^{-1} which is attributed to O–H (H-bonded) stretching. A band at 2924.52 cm^{-1} corresponds to aliphatic C-H stretching, 1633.41 cm^{-1} is related to the Amide I band which indicates the presence of (N-H) groups. The peak at 1036.55 cm^{-1} is associated with C-N stretching [7]. **Cs/AC_P** showed a peak at 3432.67 cm^{-1} due to the O–H (H bonded) stretching, that at 2923.56 cm^{-1} is due to the typical asymmetric and symmetric stretching C-H stretch vibrations, and at 1634.38 cm^{-1} and 1035.59 cm^{-1} were assigned to N-H bending and C-N stretching, respectively [7].

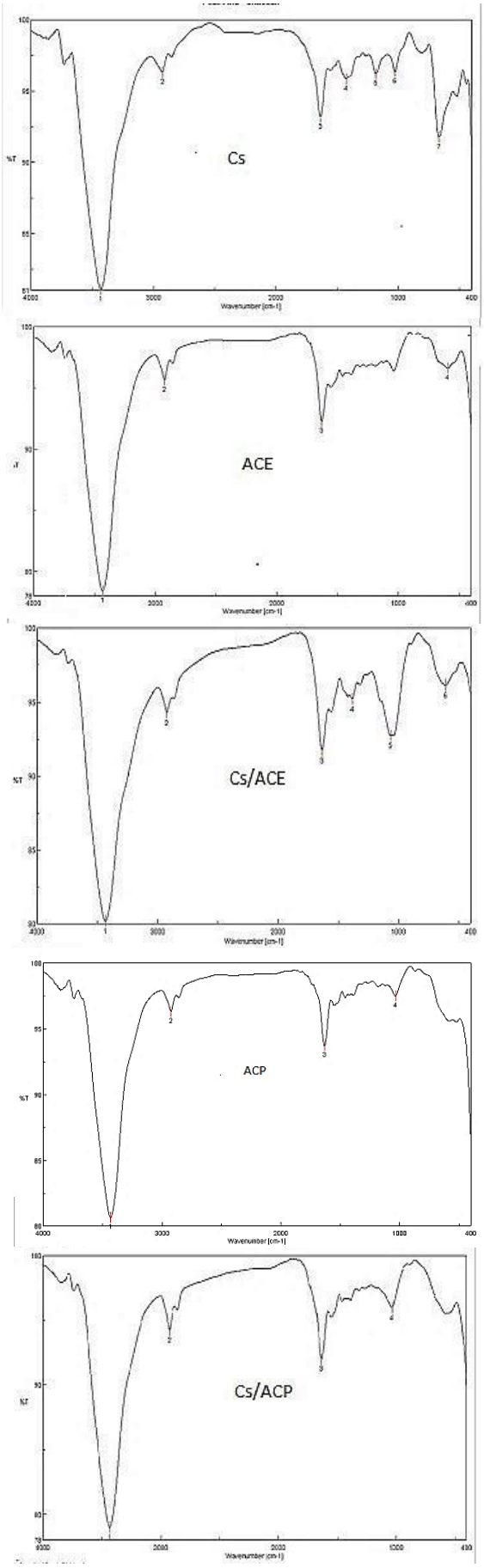

Fig.2. FTIR spectra for Cs, AC_E, AC_P, Cs/AC_E and Cs/AC_P.

3.2. The effect of adsorbent weight

Figure 3 shows the effect of varying the adsorbent dose of Cs, Cs/AC_p and Cs/AC_P upon the removal of AB and MV from solution. The results indicated that the removal % increased with the increase in adsorbent dose from 0.0125 to 0.1 g. A further increase in all adsorbents weights after 0.05 g showed no significant affect in the adsorption efficiency due to reaching an equilibrium between the adsorbent and adsorbate [14]. The data revealed that AB removal% (C_o= 30 mg/L) reached 88%, 90% and 89.3% using 0.1 g of Cs, Cs/AC_p and Cs/AC_P, respectively. Previous studies reported that 93% AB removal was achieved using 0.2 g of adsorbent using an initial C_o=20 mg/L [15].

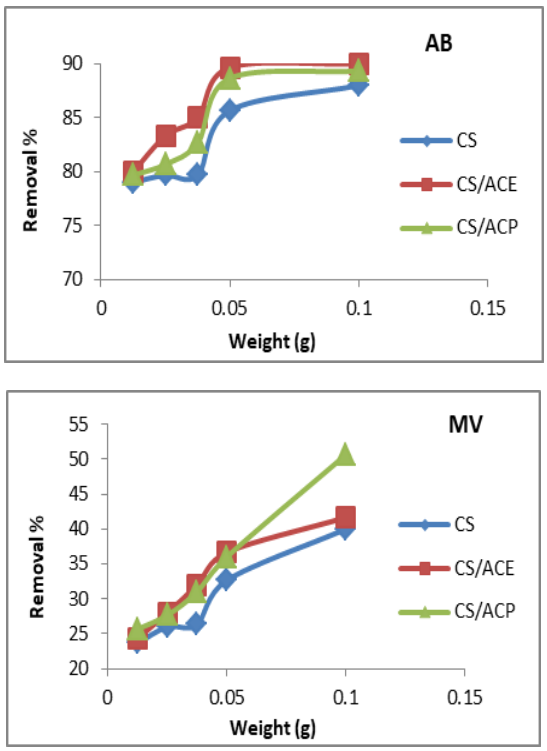

Fig. 3. The effect of adsorbent weight upon AB and MV removal using Cs, Cs/AC_E and Cs/AC_P (pH=5, vol=50 mL, time= 2 h, C_o=30 mg/L).

3.3. Effect of initial pH

The effect of initial pH upon the removal % of AB and MV using Cs, Cs/AC_E and Cs/AC_P is shown in **Figure 4**. For AB, the figure shows that the maximum removal was achieved at pH_5. This may be attributed to the dye pk_a (pk_a=4.6) and as the solution pH exceeds this value, protonated AB molecules existed in the solution. When the pH value of the solution was lower than 4.6, AB protonated molecules become ionized to the positively charged anilinium ions [15]. On the other hand, maximum removal of MV was obtained at pH_5 higher than the dye's pk_a=0.9. The minimal removal of MV at pH_1 may be attributed to the presence of excess H^+ ions which competed with the dye cation groups for the adsorption sites. However, the increase MV removal at higher pH values may be due to the enhanced association of the dye cations to the adsorbent surface favored by electrostatic attraction forces [16].

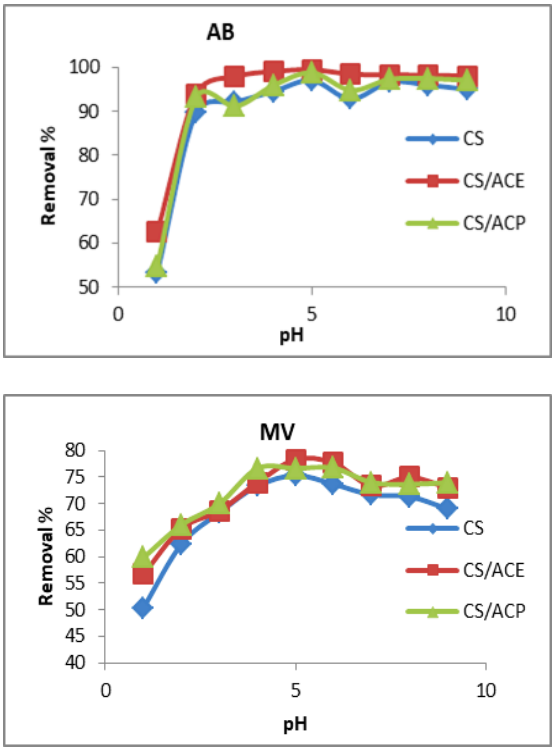

Fig.4. The effect of initial pH on AB and MV removal using Cs, Cs/AC_E and Cs/AC_P at (adsorbent weight =0.1 g, vol =50 mL, time= 2h, C_o=30 mg/L).

3.4. Effect of initial concentration

The effect of AB and MV initial concentration upon its removal using Cs, Cs/AC_E and Cs/AC_P is shown in **Figure 5**. It was observed that the AB and MV % removal decreased with the increase in the initial dye concentration from 10 to 150 mg/L. This may be due to the fact that at lower concentrations the ratio of the initial number of AB and MV molecules to the available adsorption sites was low and, subsequently, more adsorption sites were available [17]. As the initial dye concentration increased, the number of AB and MV

molecules also increased relative to the available adsorption sites on Cs, Cs/AC_E and Cs/AC_P and thus there was a decrease in % dye removal [18].

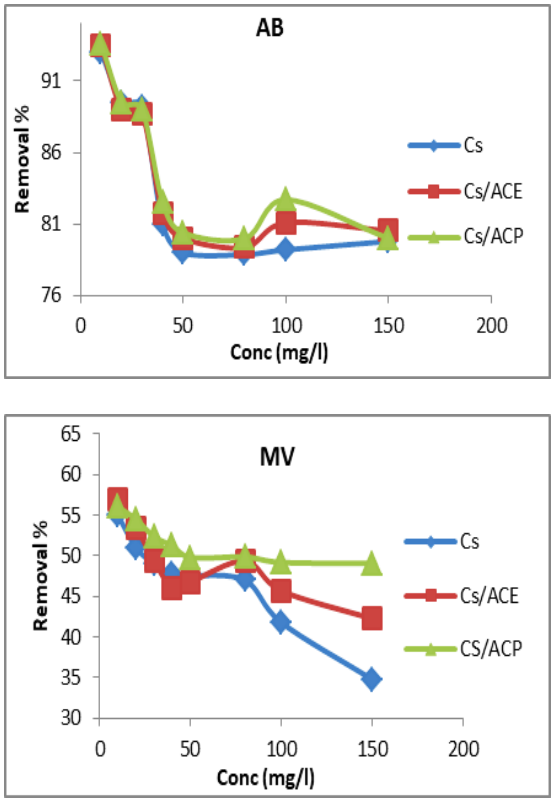

Fig.5. Effect of AB and MV initial concentration on its removal of using Cs, Cs/AC_E and Cs/AC_P (pH= 5, vol=50 mL, time= 2h, adsorbent weight=0.1 g).

3.5. Effect of contact time

Dye removal using Cs, Cs/AC_E and Cs/AC_P was investigated at different contact time. The results are shown in **Figure 6**. It is evident from the results that increasing the time from 15 to 300 min lead to a rapid increase in adsorption efficiency for AB and MV dye onto the prepared adsorbents. However, increasing the contact time beyond 300 min, the adsorption efficiency remained constant indicating equilibrium was reached due to saturation of the adsorbent active sites [7].

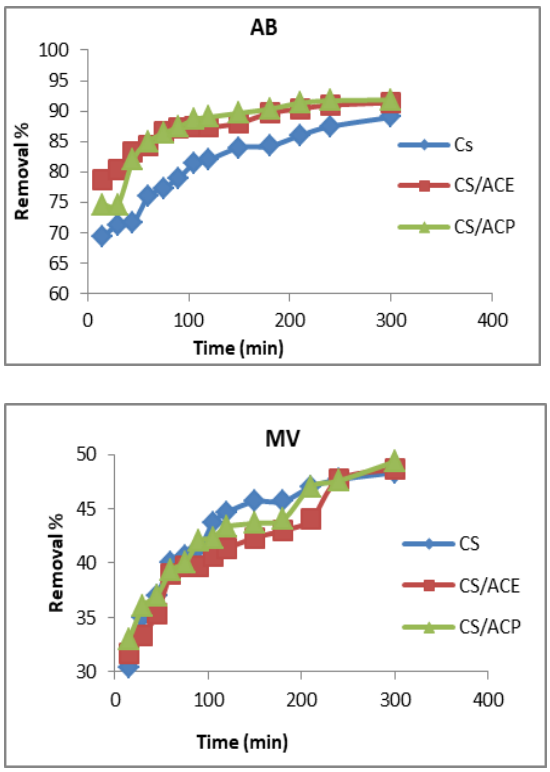

Fig.6. Effect of contact time upon AB and MV removal % using Cs, Cs/AC_E and Cs/AC_P (pH= 5, vol=50 mL, initial concentration=30 mg/L, adsorbent weight=0.1 g).

Adsorption Kinetics:

Tables 1 and **2** show the kinetic parameters for the AB and MV adsorption onto Cs, Cs/AC_E and Cs/AC_P applying Lagergren pseudo-first-order, pseudo-second-order rate equation and intra-particle diffusion equations. From the data, it was shown that the adsorption of both dyes fitted well the pseudo-second-order kinetic model as indicated by R^2values. The intra-particle diffusion parameter describes the diffusion mechanism and rate controlling steps [19]. The correlation coefficient (R^2) values for intra-particle diffusion models were significant and the plot gave a value for the intercept. This intercept value indicates that the lines did not pass through the origin, signifying that adsorption involved intra-particle diffusion after an initial stage where the dye got adsorbed onto the surface of the adsorbent.

Table 1. Kinetic models parameters for the adsorption AB onto Cs, Cs/AC_E and Cs/AC_P.

Adsorbent	Pseudo first order			Pseudo second order			Intra-particle diffusion model		
	qe(mg/g)	$k_1(min^{-1})$	R^2	qe(mg/g)	k_2 (g/mg.min)	R^2	$k_3(mg\ g^{-1}\ min^{-1/2})$	C (mg g^{-1})	R^2
Cs	2.77	0.01	0.894	13.65	227.7	0.999	0.235	9.52	0.967
Cs/AC_E	1.69	0.006	0.808	13.88	506.1	0.999	0.141	11.51	0.920
Cs/AC_P	1.98	0.008	0.671	14.06	448.4	0.999	0.198	10.87	0.815

Table 2. Kinetic models parameters for the adsorption MV onto Cs, Cs/AC_E and Cs/AC_P

Adsorbent	Pseudo first order			Pseudo second order			Intra-particle diffusion model		
	qe(mg/g)	$k_1(min^{-1})$	R^2	qe(mg/g)	$k_2(min^{-1})$	R^2	$k_3(mg\ g^{-1}\ min^{-1/2})$	C ($mg\ g^{-1}$)	R^2
Cs	2.16	0.008	0.788	7.89	16.24	0.999	0.192	4.29	0.912
Cs/AC_E	2.45	0.008	0.904	8.47	20.02	0.993	0.182	4.16	0.959
Cs/AC_P	2.19	0.007	0.906	7.86	19.81	0.996	0.174	4.45	0.973

Adsorption isotherm

Langmuir, Freundlich and Dubinin-Radushkevich isotherm models have been shown to be suitable for describing short-term and mono component adsorption of dyes by different biosorbent materials. Essentially, Langmuir isotherm model assumes a monolayer for adsorption onto the surface occurs assuming a certain sum of identical sites is present. Once the active sites are occupied, no additional adsorption can occur. Freundlich model, on the other hand, is based on a multilayer for adsorption on a heterogeneous surface. Dubinin-Radushkevich model is used for estimating the mechanism of surface adsorption. **Tables 3 and 4** show the fitting parameters of the obtained data applying the three isotherm models considered. Based upon the obtained R^2 values, the adsorption of both dyes fitted the Freundlich>Langmuir>D–R. In other words, the process of AB and MV adsorption of onto Cs, Cs/AC_E and Cs/AC_P may be regarded as a physical process [20].

Table 3. Langmuir, Freundlich and Dubinin-Radushkevich isotherm parameters for AB adsorption onto Cs, Cs/AC_E and Cs/AC_P

Adsorbent	Langmuir isotherm			Freundlich isotherm			D-R isotherm		
	b ($L\ mg^{-1}$)	qe ($mg\ g^{-1}$)	R^2	K_f $mg\ g^{-1}$ ($mg\ L^{-1}$)	1/n	R^2	q(D–R) ($mg{\cdot}g^{-1}$)	E ($KJ.mol^{-1}$	R^2
Cs	0.04	83.9	0.592	5.54	0.63	0.965	25.1	1.16	0.597
Cs/AC_E	0.04	89.9	0.571	5.55	0.64	0.967	24.8	1.22	0.572
Cs/AC_P	0.04	90.2	0.601	5.69	0.64	0.969	25.1	1.23	0.581

Table 4. Langmuir, Freundlich and Dubinin-Radushkevich isotherm parameters for MV adsorption onto Cs, Cs/AC_E and Cs/AC_P

Adsorbent	Langmuir isotherm			Freundlich isotherm			D-R isotherm		
	$b(Lmg^{-1})$	$qe(mgg^{-1})$	R^2	$K_f mg\ g^{-1}$ ($mg\ L^{1}$)	1/n	R^2	q(D–R) ($mg{\cdot}g^{-1}$)	E ($KJ.mol^{-1)}$	R^2
Cs	0.01	48.81	0.958	0.916	0.76	0.986	14.3	0.27	0.672
Cs/AC_E	0.006	84.7	0.702	0.827	0.82	0.991	14.9	0.28	0.621
Cs/AC_P	0.004	156.6	0.678	0.735	0.89	0.999	16.5	0.26	0.652

3.6. Effect of temperature and thermodynamic studies

The adsorption of AB and MV onto Cs, Cs/AC_E and Cs/AC_P was studied at different temperatures (25º, 30º, 35º and 40 ºC). The results (**Figure 7**) indicated that, in general, the % removal increased as the temperature increased for both dyes. As well, adsorption of the dye molecules onto Cs, Cs/AC_E and Cs/AC_P increased significantly as the temperature was raised from 25 ºC to 40 ºC. This increase indicates that as the temperature increased, the dye molecules gained enough energy to be transported into the pores of the adsorbent. This may reflect the fact that the process of adsorption was diffusion controlled [20].

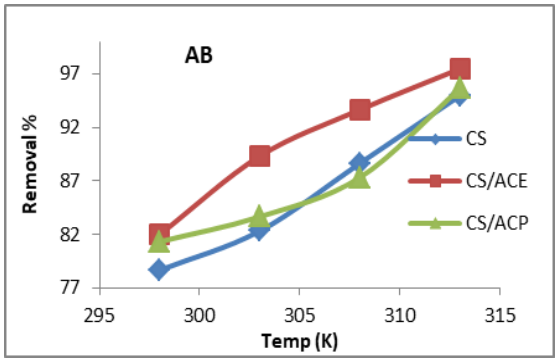

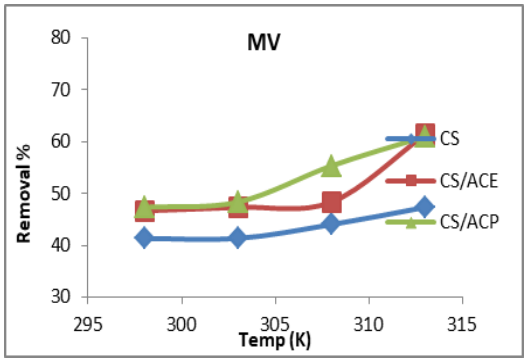

Figure 7. The effect of varying the solution temperature upon the removal % of AB and MV using Cs, Cs/AC_E and Cs/AC_P (pH= 5, volume= 50 mL, adsorbent weight =0.1 g, time=2h, C_o =30 mg/L).

Thermodynamic parameters such as standard Gibbs free energy ($\Delta G°$), enthalpy ($\Delta H°$) and entropy change ($\Delta S°$) of adsorption were calculated using the following equations [21]:

$$\Delta G^0 = RT\ln K_C$$

where R is the gas constant in kJ/mol K, T is the temperature of adsorption in K and K_c is the equilibrium constant given as

$$K_C = \frac{C_{Be}}{C_{Ae}}$$

where C_{Ae} and C_{Be} are the equilibrium concentration of the dye in solution and on the adsorbent, respectively. $\Delta H°$ and $\Delta S°$ were determined using the van't Hoff equation:

$$\ln K_C = \frac{\Delta S^0}{R} - \frac{\Delta H^0}{RT}$$

The values of the thermodynamic parameters were calculated and are shown in **Tables 5 and 6.** The data revealed that $\Delta G°$ for AB was negative which indicated that the process was spontaneous; however, it was positive for MV which indicated that the adsorption process was non spontaneous. The positive values of $\Delta H°$ indicate that the adsorption of AB and MV was endothermic and the positive values of $\Delta S°$ reflect an increase in the degree of freedom and randomness at the solid /solution surface during the adsorption process.

Table 5. Thermodynamic parameters for the adsorption of AB onto Cs, Cs/AC_E and Cs/AC_P

Temp (K)	Cs				Cs/AC_E				Cs/ACP			
	ln Kc	ΔG (J mol^{-1})	ΔH (kJ mol^{-1})	ΔS (J $mol^{-1}K^{-1}$)	ln Kc	ΔG (J mol^{-1})	ΔH (kJ mol^{-1})	ΔS (J $mol^{-1}K^{-1}$)	ln Kc	ΔG(J mol^{-1})	ΔH (kJ mol^{-1})	ΔS (J $mol^{-1}K^{-1}$)
298	0.6	-1205	80654	275	0.82	-1956	104183	356	0.8	-1592	63469	218
303	0.8	-2579			1.43	-3737			0.9	-2684		
308	1.4	-3952			2.0	-5518			1.2	-3775		
313	2.2	-5325			2.9	-7299			2.4	-4867		

Table 6. Thermodynamic parameters for the adsorption of MV onto Cs, Cs/AC_E and Cs/AC_P

Temp (K)	Cs				Cs/AC_E				Cs/ACP			
	ln Kc	ΔG ($kJmol^1$)	ΔH ($kJmol^1$)	ΔS ($Jmol^1K^1$)	ln Kc	ΔG ($kJmol^1$)	ΔH ($kJmol^1$)	ΔS ($Jmol^1K^1$)	ln Kc	ΔG ($Jmol^1$)	ΔH ($kJmol^1$)	ΔS ($Jmol^1K^1$)
298	-1.04	2664	12396	33	-0.8	2880	27303	84	-0.8	2166	35068	110
303	-1.04	2501			-0.8	1860			-0.7	1614		
308	-0.9	2338			-0.7	1440			-0.5	1062		
313	-0.8	2714			-0.2	1020			-0.2	510		

4. Conclusion

In this work, the removal of aniline blue (AB) and methyl violet (MV) from aqueous solution using chitosan (C_s) and chitosan/activated carbon biomass prepared from eggplant (C_S/AC_E) and pomegranate peels (C_s/AC_P) was investigated. The results

indicated that the prepared chitosan/ activated carbon enhanced the removal of both dyes relative to chitosan alone. The adsorption process followed the pseudo-second-order equation and fitted the Freundlich isotherm model for both dyes. Thermodynamic parameters ($\Delta H°$, $\Delta S°$ and $\Delta G°$) for the uptake of both dyes onto the used adsorbents indicated that the process was endothermic and spontaneous for AB, and non-spontaneous for MV.

References

1. C Namasivayam, D Prabha and M Kumutha, (1998) Removal of Direct Red and Acid Brilliant Blue by Adsorption on to Banana Pith, Bioresource Technology **64** 77-79.
2. W Wei , G L Yan, W H Zhong, S Y Li , Cui J and Z G Wei, (2015),Fast Removal Of Methylene Blue From Aqueous Solution By Adsorption Onto Poorly Crystalline Hydroxy apatite Nanoparticles, Digest *Journal of Nanomaterials and Biostructures* Vol. 10, No. **4**, p. 1343- 1363.
3. A A Inyinbor, F A Adekola and G A Olatunji, Kinetics, (2016) isotherms and thermodynamic modeling of liquid phase adsorption of Rhodamine B dye onto Raphiahookerie fruit epicarp, Water Resources and Industry **15**: 14–27.
4. A Azimi, A Azari, M Rezakazemi and M Ansarpour,(2017) , Removal of Heavy Metals from Industrial Wastewaters, Chem BioEng Rev **4**, No. 1, 1–24
5. A A Moosa, A M Ridha and N A Kadhim, (2016), Use of Biocomposite Adsorbents for the Removal of Methylene Blue Dye from Aqueous Solution, American *Journal of Materials Science* **6(5):** 135-146.
6. M A Aseel, N A Abbas and F A Ayad, (2017) Kinetics and equilibrium study for the adsorption of textile dyes on coconut shell activated carbon, Arabian *Journal of Chemistry* **10**, S3381–S3393.
7. R Han, Y Wang, W Zou, Y Wang and J Shi, (2007) Comparison of linear and nonlinear analysis in estimating the Thomas model parameters for methylene blue adsorption onto natural zeolite in fixed-bed column, *Journal of Hazardous Materials* **145** 331–335.
8. M Eddebbagh, A Abourriche, M Berrada, M Ben Zina and A Bennamara, (2016) Adsorbent material from pomegranate (*Punicagranatum*) leaves: Optimization on removal of methylene blue using response surface methodology, JMEC, Sci. **7 (6)** 2021-2033.
9. S Hydari, H Sharififard, M Nabavinia and M R Parvizi, (2012) A comparative investigation on removal performances of commercial activated carbon, chitosan biosorbent and chitosan/activated carbon composite for cadmium, *Chemical Engineering Journal* **193**–194 276–282.
10. Rahmi, (2018), Preparation of chitosan composite film using activated carbon from oil palm empty fruit bunch for Cd2+ removal from water, IOP Conference Series: Materials Science and Engineering, pp. 1-8.
11. A Venault, L Vachoud, C Pochat, D Bouyer and C Faur, (2008) Elaboration of chitosan/activated carbon composites for the removal of organic micropollutants from Waters, Environ. Technol., 29 1285.
12. R Subha and C Namasivayam, (2009),Zinc chloride activated coir pith carbons as low cost adsorbent for removal of 2,4- dichloro phenol: Equilibrium and kinetic studies. Indian *journal of chemical technology*. Vol. **16**, November pp. 471-479.
13. L A Awin, M A El-Rais, A M Etorki, N A Mohamed and W A Makhlof, (2018), Removal of Aniline Blue from Aqueous Solutions Using Ce1−xBixCrO3 (x = 0, 0.5, 1), Open *Journal of Inorganic Non-metallic Materials*, **8**, 1-10.
14. B K Aziz, D M Salh, S Kaufhold and P Bertier , (2019),The High Efficiency of Anionic Dye Removal Using Ce-Al13/Pillared Clay from Darbandikhan Natural Clay, Molecules 24, 2720, p 1-15.
15. Q Liua , B Yangb , L Zhanga and R Huanga, (2015) Removal of aniline from aqueous solutions by activated carbon coated by chitosan, , *Journal of Water Reuse and Desalination* **5 (4)**: 610-618.
16. Z Muhammad, (2012),Removal of Crystal Violet from Water by Adsorbent Prepared from Turkish coffee Residue, ENVIRONMENTAL CHEMISTRY, pp 107-113.
17. M Wawrzkiewicz and Z Hubicki, (2010) Equilibrium and kinetic studies on the sorption of acidic dye by macroporous anion exchanger, *Chemical Engineering Journal* 157 29–34.
18. G H Sonawane and V S Shrivastava, (2008) Utilization of bioadsorbent based on zeamaize for removal of water soluble dye: The Kinetic Studies, Ajcer. **1**, 19–27.

19. A Balouch, M Kolachi, F N Talpur, H Khan and M I Bhanger, Sorption Kinetics, (2013) Isotherm and Thermodynamic Modeling of Defluoridation of Ground Water Using Natural Adsorbents, Sci. Res**. 4** 221-228.
20. P K Pandey, S Choubey, Y Verma, M Pandey, S S K Kamal and K C shekhar, (2007),Biosorptive Removal of Ni (II) from Wastewater and Industrial Effluent. *Int. J. Environ. Res. Public Health*, **4(4)**, 332-339.
21. M Hema and S Arivoli, (2007) Comparative study on the adsorption kinetics and thermodynamics of dyes onto acid activated low cost carbon, *Int. J. Phys. Sci*. **2**, 10–17.